

Karhunen-Loeve mode control of chaos in a reaction-diffusion process

Ioana Triandaf^{1,*} and Ira B. Schwartz²

¹*Science Applications International Corporation, Applied Physics Operation, McLean, Virginia 22102*

²*U.S. Naval Research Laboratory, Special Project for Nonlinear Science, Code 6700.3, Plasma Physics Division, Washington, DC 20375-5000*

(Received 10 December 1996)

We introduce a chaos control method that stabilizes unstable states of a spatiotemporal process based on analyzing the dynamics of the main coherent structure in the data represented by the highest energy Karhunen-Loeve mode. The problem is then reduced to the application of embedding techniques to the control of a time series given by the amplitude of a dominant spatial mode. The algorithm is applied to a reaction-diffusion process where we stabilize an unstable orbit inside a chaotic regime. One advantage of the control procedure is that it is independent of sensor placement. Furthermore, we find the desired control state is achieved exponentially, and the procedure can be applied directly to experimental data. [S1063-651X(97)01407-4]

PACS number(s): 05.45.+b, 82.20.-w, 82.40.Bj

I. INTRODUCTION

Chaos control based on variations of the technique presented in [1] has now been applied to many experiments in many different fields of science [2]. Successful control for many of these experiments occurs mostly for low dimensional dynamical systems. Some of these low dimensional systems may be embedded in high dimensional spaces, and occur in continuous spatiotemporal systems governed by nonlinear partial differential equations. Examples of some of the applications possessing low dimensional but unstable behavior include periodic and steady state behavior in nonlinear multimode lasers [3], steady motion in Rayleigh-Bénard convection [4], and traveling waves in wide aperture lasers [5] and plasma discharge tubes [6].

In this paper, we are interested in stabilizing unstable states and eliminating chaos in a spatiotemporal process by using the natural dynamics of the system; i.e., we wish to control chaos based on exploiting stable manifolds already present in the data. This type of control is based on a geometric model constructed directly from data obtained by well-known embedding techniques [7,8]. The geometric model contains important information about the flow, such as attractors and stable and unstable manifolds, and replaces the equations of state with an approximate model of phase space. The control amounts to finding suitable states in the given data and using parameter adjustments to maintain the system on a desired state by directing the process to stable manifolds that can be identified from data. This approach to chaos control was initiated by Ott, Grebogi, and Yorke [1], and has been extended to allow the controlled state to be maintained as parameters are varied [9,10], i.e., track, or continue, the controlled state as a function of parameters. The combination of control and tracking has been successful in stabilizing low dimensional attractors modeled by both low and high dimensional equations of state; see, for example, the experiments

in [11,3]. The next step was to address processes that are continuous in space, such as those used in modeling bursting in reaction-diffusion processes.

In [12], the authors have introduced an algorithm for controlling unstable states of a spatiotemporal process and applied it to the same reaction-diffusion system presented in this paper. It is a generic model that reproduces the spatiotemporal two-front bursting patterns observed for a chlorite-iodide reaction in the Couette flow reactor. It provides rich dynamics, most of which have been observed experimentally [13,14]. The chaotic and intermittent bursting regime we address is likely to be observed in certain experiments [15]. The algorithm introduced in [12] was based on sampling the data in the most active region at a fixed spatial point. Time series embedding methods were then used to analyze the dynamics at the fixed spatial point. Control was then implemented by adjusting the flow-feed rate at the boundary to maintain the system on the stable manifold of a desired orbit.

The main drawback to spatiotemporal control of low dimensional objects using the adaptive time series from a single point is that it may be extremely sensitive to measurement location. Other control techniques that are nonadaptive also suffer from spatial location measurement problems. In [6], the total success of control using a fixed delay and gain is highly dependent on where the probe is placed. In part, this is due to uncorrelated regions in space of the dynamics. It may also be a result of low energy output of the signal in certain spatial regions. It is the purpose of this paper to attempt to provide a partial solution to this problem for spatiotemporal systems.

In this paper we propose an alternate control algorithm based on analyzing the dynamics of the dominant coherent structures contained in a spatiotemporal pattern of the system. We decompose the chaotic solution of the reaction-diffusion system into its main coherent structures also known as Karhunen-Loeve (KL) modes or empirical eigenfunctions [16]. These are structures that best approximate the solution in the mean square sense. The most dominant structure is the one that when properly normalized and projected back onto the solution yields the maximum mean square energy, and can therefore be thought of as the most representative spatial structure in a statistical sense. Repeated application of the

*Mailing address: U.S. Naval Research Laboratory, Special Project for Nonlinear Science, Code 6700.3, Plasma Physics Division, Washington, DC 20375-5000.

procedure yields a complete hierarchy of structures ranked according to their mean square energy content. Such a set of modes describes an optimal coordinate system with respect to the data. An important property is that these modes are uncorrelated, which may be interpreted as each mode representing a statistically independent object. As shown in [17] the modes may be an efficient means of representing the data, rather than Fourier modes. The KL modes allow for compact representation of the data and may be used for data compression and development of low-dimensional models [18,17]. It would therefore be of interest to investigate the possibility of controlling a spatiotemporal process based on monitoring its main coherent structures, since the measurable signal information is most likely captured in the most energetic modes.

For the reaction-diffusion model we consider, we have found that control based on monitoring the dynamics of the highest energy KL mode stabilizes the whole spatial process. Compared to our previous control method [12], this method locks on the desired state exponentially fast, and since projection of the spatiotemporal solution on a KL mode is involved, we eliminate the problem of choosing an appropriate domain location for sampling the data. In the previous method, control had to be based on observing the dynamics in the most active region.

A method similar in spirit was introduced in [19] for monitoring ignition and extinction in a catalytic wafer for exothermic oxidation reactions. Projection on the main KL mode is used in a state variable control method to maintain the system in a stable state with a small basin of attraction that is destabilized by noise. Our method also observes the amplitude of the main KL mode with the difference that we use it for parameter control to maintain states that are unstable. Essential to our method is the constructive use of the local dynamics by embedding techniques in addition to observing the projection of the data on the main KL mode.

This paper is organized as follows: in Sec. II we present the reaction-diffusion model. Then we review in Sec. III the Karhunen-Loeve procedure. In Sec. IV we introduce the algorithm and in Sec. V we give numerical examples. We end the paper with a discussion section.

II. THE MODEL

We consider the following one-dimensional reaction-diffusion system:

$$\frac{\partial u}{\partial t} = D \frac{\partial^2 u}{\partial x^2} + \frac{1}{\epsilon} [v - f(u)], \quad (1a)$$

$$\frac{\partial v}{\partial t} = D \frac{\partial^2 v}{\partial x^2} - u + \alpha, \quad x \in [0,1],$$

subject to Dirichlet boundary conditions:

$$u(x=0,0) = u_0, \quad v(x=0,0) = v_0 \quad (1b)$$

$$u(x=1,0) = u_0, \quad v(x=1,0) = v_0.$$

Parameters ϵ and α are assumed positive and fixed. The choice of the Van der Pol-like reaction term determines the types of patterns that form. In [20] a wide range of patterns is

presented for different choices of nonlinear function f . The dynamics becomes more complex as $D \rightarrow 0$, and the patterns for small diffusion are more difficult to realize experimentally as well as numerically. The observed patterns include stationary and oscillating single-front and multiple-front patterns as well as patterns in which single- and multiple-front patterns alternate. These generic patterns can be observed in any reaction-diffusion system regardless of the physical phenomenon it models, depending only on the existence of the S-shaped slow manifold governed by the nonlinear function f [15].

For our method we will consider the two-front pattern with two diffusion-dominated regions at the boundaries and chaotic bursting occurring in the middle region (Fig. 1). The nonlinear term we consider is given by $f(u) = u^2 + u^3$, and ensures the existence of an S-shaped slow manifold consisting of three branches. The upper and lower branches attract the trajectories in a time of order $1/\epsilon$. The chaos observed for this system consists of small amplitude chaos that takes place on the middle branch of the manifold with chaotic large amplitude bursts when the dynamics visits the upper branch. The remarkable feature of this chaotic pattern is that it could not be observed in the absence of diffusion, and the chemical reaction itself would evolve in a steady manner [20].

III. KARHUNEN-LOEVE DECOMPOSITION

In this section we describe briefly the KL decomposition applied to a chaotic spatiotemporal pattern of the reaction-diffusion model presented above. This is a procedure of mode expansion for spatiotemporal processes that extracts the relevant degrees of freedom of the dynamics of a large data set. The modes are defined by the data and constitute a natural coordinate system that approximates the data optimally in the L^2 norm. The modes are orthogonal, accounting for spatially independent features of the data. The procedure is associated with the names of Karhunen [21] and Loeve [22] and was first applied to spatiotemporal dynamics by Lorenz [23], for weather prediction, under the name of proper orthogonal expansion, and by Lumley [24], for the study of fluid turbulence problems. (See [25] for a review of the KL method and turbulence.)

The procedure applies to a discretized spatiotemporal pattern, say a solution of Eq. (1), $\mathbf{u}(x,t) = (u(x,t), v(x,t))$, given in terms of a computational spatial grid $\mathbf{x} = (x_1, \dots, x_p)$, and at discrete intervals in time $\{t_n\}$:

$$\{u^n(x)\} = \{\mathbf{u}(x, t_n)\}_{n=1, M}. \quad (2)$$

The KL eigenmodes are the eigenfunctions of the auto-correlation matrix $K(x, x')$. This matrix is given by

$$K(x, x') = \langle \mathbf{u}(x, t) \mathbf{u}(x', t) \rangle,$$

where the brackets stand for time average and the vector product is the dyadic product. Explicitly an element in $K(x, x')$ is given by

$$K_{ij} = \frac{1}{M} \sum_{n=1}^M (u(x_i, t_n)u(x_j, t_n) + u(x_i, t_n)v(x_j, t_n) + v(x_i, t_n)u(x_j, t_n) + v(x_i, t_n)v(x_j, t_n)). \quad (3)$$

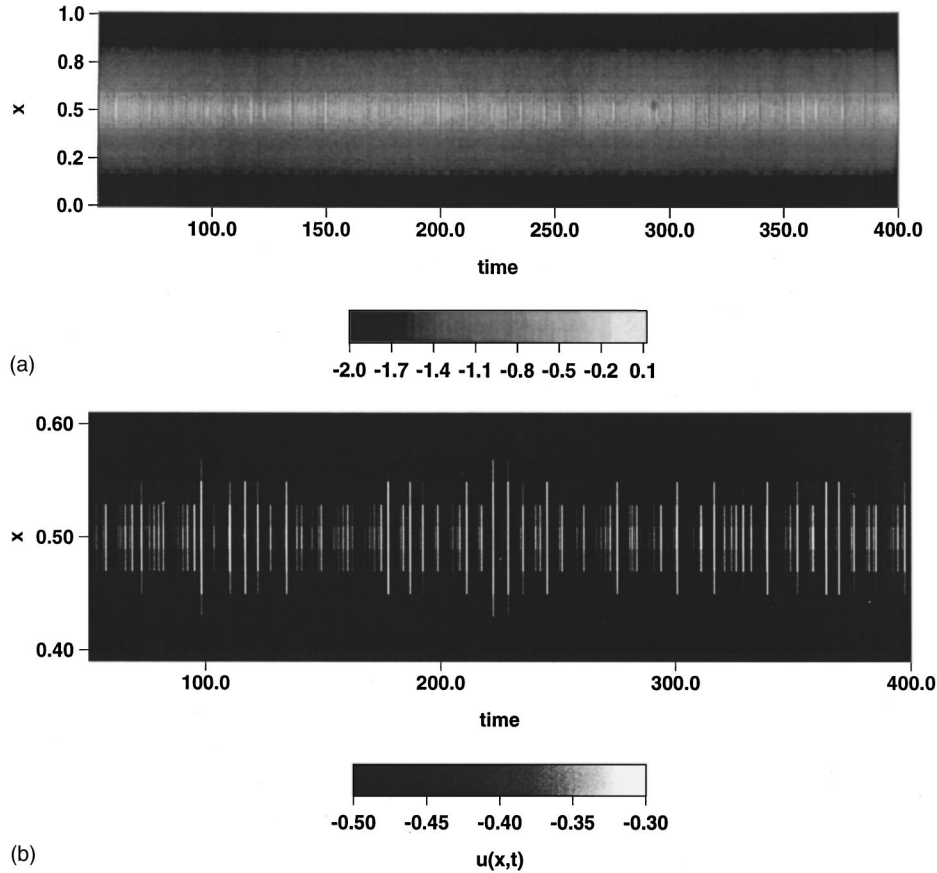


FIG. 1. (a) Spatiotemporal pattern for the u variable (dimensionless units) in the reaction-diffusion model. These data were expanded in KL modes. Parameter values used here are $D = 0.032249$, $\alpha = 0.1$, $\epsilon = 0.1$. Boundary conditions are $u(0,t) = u(1,t) = -2$, $v(0,t) = v(1,t) = -4$. (b) Detailed view of the pattern in Fig. 1(a).

The field \mathbf{u} may be expanded as

$$\mathbf{u}(x,t) = \sum_n \alpha_n(t) \psi_n(x), \quad (4)$$

where the amplitudes of the KL modes are orthogonal in time:

$$\langle a_n(t) a_m(t) \rangle = \lambda_n \delta_{nm},$$

where the left term is a time average. So, in this representation, the Fourier coefficients $a_n(t)$ are decorrelated. As a result, when projecting the data (2) back onto each eigenmode we get uncorrelated time series from each mode, representing statistically independent phenomena. An eigenvalue of \mathbf{K} may be written as

$$\lambda_n = \frac{(\psi_n, \mathbf{K} \psi_n)}{\|\psi_n\|^2} = \langle |(\psi_n, \mathbf{u})|^2 \rangle,$$

where the angular brackets stand for time averaging, so a KL eigenvalue may be interpreted as giving the mean energy of the system projected on the corresponding eigenmode.

The KL modes, i.e., the eigenfunction of K , can be obtained equivalently by a minimization procedure [16,26]. To find the first eigenmode of a given data set, one determines the one spatial structure, which when properly normalized and projected onto the data yields the maximum mean square energy, so it is the most representative structure in a statistical sense. Once this eigenmode is found, we find the second mode by repeating the procedure for $\mathbf{u} - \alpha_1 \psi_1(x)$ continuing

this process. This yields a hierarchy of spatial structures ranked according to mean square energy content, determined by the data itself.

In practice, determining the eigenfunctions of the correlation matrix creates computational difficulties due to the large size of the matrix K . An alternate method to compute the KL modes by which one can reduce the size of the matrix involved is the method of snapshots due to Sirovich [16]. This method consists in determining the eigenfunctions of K , as a combination of the time snapshots with coefficients depending on time:

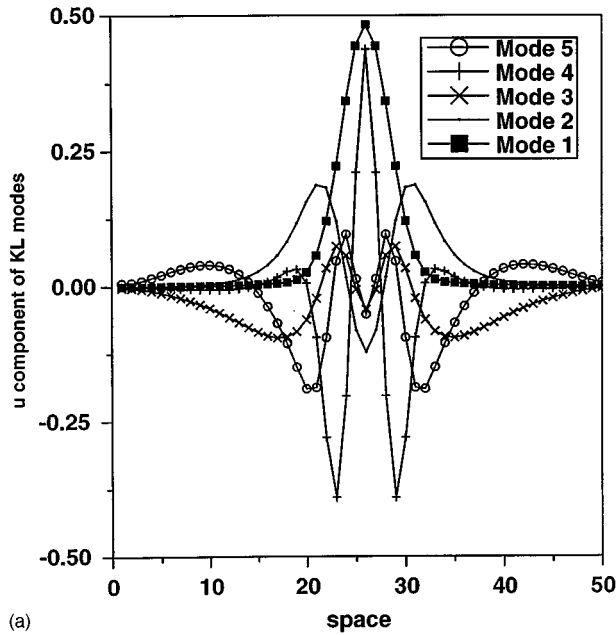
$$\Psi(x,t) = \frac{1}{M} \sum_{k=1}^M \alpha_k(t) \mathbf{u}_k(x).$$

These coefficients are determined as eigenvalues of a time correlation matrix C with elements

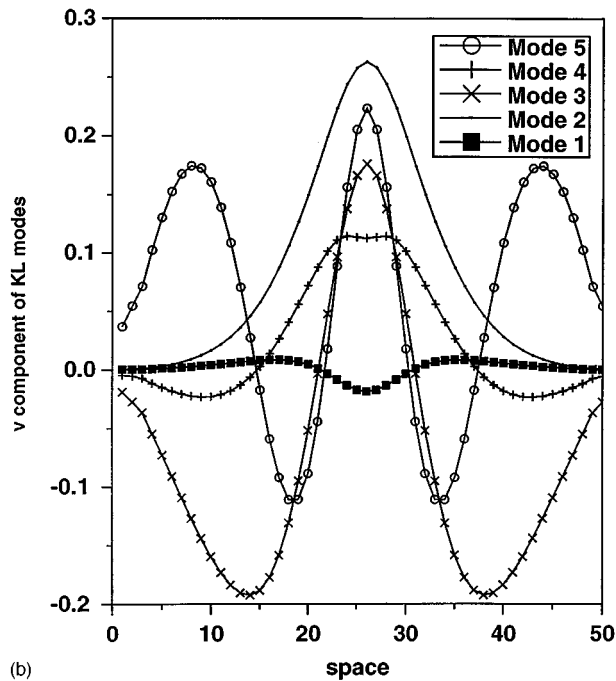
$$C(t,s) = \langle \mathbf{u}(x,t) \mathbf{u}(x,s) \rangle,$$

where N is the number of spatial mesh points. C is an $M \times M$ matrix, where M is the number of time snapshots.

We performed KL decomposition on a chaotic solution of the system (1). The pattern for the u variable is shown in Figs. 1(a) and 1(b) and consists in two diffusion-dominated regions at the boundaries separated by a reaction-dominated region where chaotic bursting occurs. This two-front pattern simulates phenomena in a Couette flow reactor occurring as a result of diffusion interacting with the chemical reaction when the mass transport is weak compared to diffusion.



(a)



(b)

FIG. 2. The five-highest energy KL modes. (a) u components. (b) v components (dimensionless units).

In Fig. 2 we show the five highest energy KL modes obtained by applying the procedure to the a chaotic solution of Eq. (1), (u, v) , where the u component is shown in Fig. 1(a). The highest energy mode contains 94% of the total energy, the second highest energy mode contains 5%, and the other three modes below 0.1%.

In Fig. 3 we show a color map for the coefficients of the correlation matrix corresponding to the pattern in Fig. 1(a). The regions with coefficients close to 1 in absolute value represent regions with strong correlation. Both the horizontal and vertical axes represent space. We notice that near the boundaries, in the regions where diffusion dominates, the data are strongly correlated. We also see that in the middle of the interval, where the process is mainly due to the chemical

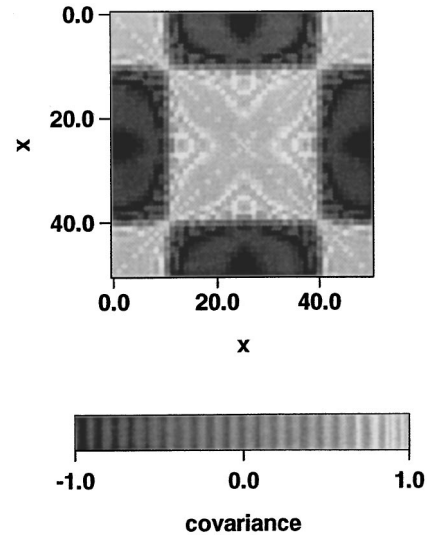


FIG. 3. Grey scale map of the correlation matrix obtained from the data in Fig. 1. Regions with the same shade stand for spatial regions where data are strongly correlated.

reaction, the data are strongly correlated. However, diffusion and reaction regions are uncorrelated with each other. So when sampling a single time series for control, the probe has to be placed in the reaction-dominated region [12]. Placing a probe in the diffusion-dominant regime and measuring a time series produces very little signal. In practice, any noise in the system would dominate the signal, impeding the acquisition of information for control.

IV. THE KL MODE CONTROL ALGORITHM

The algorithm we present stabilizes unstable states of a spatiotemporal process modeled from experimental data. The dynamics is reconstructed and unstable states are identified together with the local linear structure, directly from data. Control is achieved by adjusting an accessible parameter based on monitoring the amplitude of the highest energy Karhunen-Loeve modes.

The algorithm addresses spatiotemporal data, such as a solution of the reaction-diffusion system (1), or in general any spatiotemporal pattern obtained from experimental measurements. The first step is to find a representation of the dynamics, enabling one to identify orbits that are of interest for control. For this we use the embedding methods, which allow one to recover the phase-portrait information directly from data without first obtaining an analytical model. Essentially these techniques amount to taking appropriate time series and building a geometric model from it, in an appropriate space, in such a way that the differential structure near the orbits to be controlled is preserved. In this way the nature of the dynamical objects in the original phase space, such as stable and unstable manifolds, is preserved.

The embedding methods have been initially designed for processes depending only on time. When the data depend also on space the issue is how to sample it in space and what time series to extract from the spatiotemporal data to reconstruct the dynamics. This will depend in general on the specific process under consideration. Moreover, for the purpose of control, we need to find information only about the local

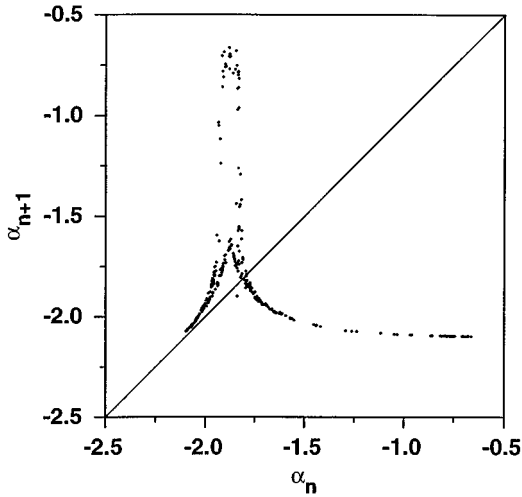


FIG. 4. First return map of the maxima of $\alpha(t)$, the amplitude of the first KL mode (dimensionless units).

dynamics near an orbit of interest. In [6] a case is shown of chaos in tube discharge, where the dynamics has to be sampled at a fixed spatial point, namely, near the cathode, in order to achieve control and eliminate chaos in the entire tube. In a previous paper [12] the authors have introduced a method for stabilizing unstable states of the reaction-diffusion system (1). In that method, in order to achieve control, we sampled the dynamics at a single spatial point. The point had to be chosen anywhere in the reaction-dominated regime, i.e., in the middle third of the unit interval in Fig. 1(a). Due to strong correlation in space, it sufficed to sample a single time series and address the dynamics of that time series in order to achieve control of the entire spatiotemporal pattern. If we sample in the diffusion-dominated region and apply the same procedure the algorithm fails.

As shown also in [19] the appropriate sampling in space is always an important issue for control. In the alternate method we propose here, we eliminate this problem by taking as our time series the amplitude of the highest energy KL mode and using it to analyze the dynamics. This time series contains information on the statistically most representative spatial structure. This is the term $\alpha_1(t)$ in the expansion (4). By construction, the highest energy KL mode is the one structure that best approximates the spatiotemporal pattern in L^2 norm. For the system (1) the highest energy KL mode contains 90% of the energy. Heuristically, that means that about 90% of the data, in time, lies close to this mode, which is shown in Fig. 2. By using this approach of sampling the dynamics, we essentially approximate \mathbf{u} by the first term in the expansion (4).

We further reduce the dimension of the sampled dynamics by sampling the chosen time series discretely, for example, at the successive maxima. This gives a map of the form

$$\alpha_{n+1} = F(\alpha_n, p),$$

where p is the control parameter and α_n denotes the successive maxima of $\alpha_1(t)$. The control parameter will be taken to be one of the Dirichlet boundary conditions. So we control by adjusting the feed rate at one of the boundaries. The map F is shown in Fig. 4 where we identify a period-one unstable

orbit in the dynamics. The data in Fig. 4 constitute the geometric model we use for control. From these data we identify the stable and unstable directions associated with the period-one unstable orbit that we need in order to apply a control algorithm. As our linear control algorithm, we used the Ott-Grebogi-Yorke (OGY) control method, which consists in changing the parameter at each iteration of the map F , so that the next iterate will fall on the stable manifold of the orbit we want to stabilize. The orbit to stabilize is a period-one saddle of the map F , which we denote by u_0 , i.e., $\alpha_0 = F(\alpha_0, p)$. This would correspond to a periodic function $\alpha(t)$ and a time-periodic pattern of the original solution of (u, v) of Eq. (1). From the data it is possible to determine the eigenvalues and eigenvectors of an orbit, for example, by using a least square fit for data near the desired orbit. Knowing such quantities, linear control can be applied. For a two-dimensional map F , with stable and unstable eigenvalues λ_s and λ_u , the OGY technique requires the parameter change

$$\delta p_n \equiv \frac{\lambda_u \xi_n \cdot \mathbf{f}_u}{(\lambda_u - 1) \mathbf{g} \cdot \mathbf{f}_u}, \quad (5)$$

where ξ is the distance from the current iterate to the orbit chosen for control, \mathbf{f}_u is the contravariant vector corresponding to the unstable direction, and the vector \mathbf{g} is the derivative of the unstable state u_0 with respect to the parameter p . g can also be determined from data by knowing the orbit at two nearby values of p .

For our system, the map F is nearly one dimensional, which amounts to $\lambda_s = 0$, in which case formula (5) becomes

$$\delta p_n \equiv \frac{\lambda_u [\alpha_n - \alpha_0(p)]}{(\lambda_u - 1) g}. \quad (6)$$

Summarizing the method consists in monitoring the amplitude of the highest energy KL mode and adjusting the control parameter every time it goes through a local maxima, according to Eq. (6). The adjusted value of the parameter is fed back into the partial differential equation solver at every maxima of $\alpha_1(t)$ and the equation is integrated in time until a new maximum is reached. We make note here that although the dynamics and control representations in Eqs. (5) and (6) are discrete, the parameter fluctuations at the boundary are not pulses similar to δ functions. Rather, the boundary condition is turned on at one maximum, and left on until the next maximum, at which point it is adjusted based on Eq. (6).

V. NUMERICAL EXAMPLES

We apply the above method to the data obtained as a numerical solution of the system (1), with $f(u) = u^2 + u^3$. The u component of this solution is shown in Fig. 1. The middle region exhibits chaotic bursting in time. We show in Fig. 5 the time series in this pattern at $x = \frac{1}{2}$. As we see from Fig. 5 the solution exhibits small amplitude chaotic oscillations of random length, all of which take place on the middle unstable branch of the nullcline. These small amplitude oscillations are followed by a large amplitude burst when the

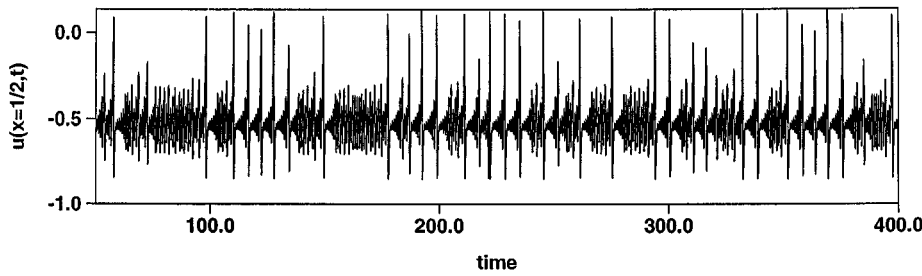
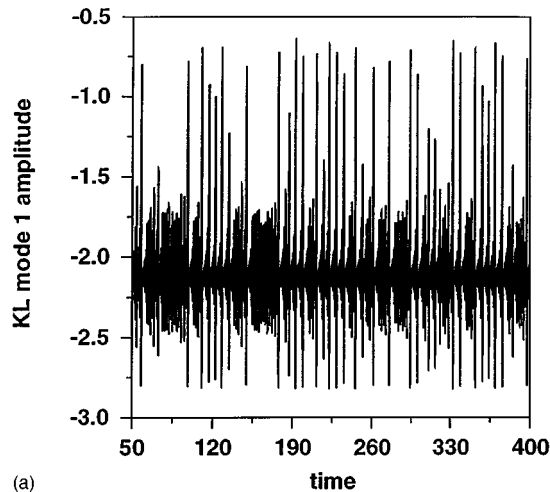


FIG. 5. Time series for u recorded at $x = \frac{1}{2}$ and $p = -2.0$.

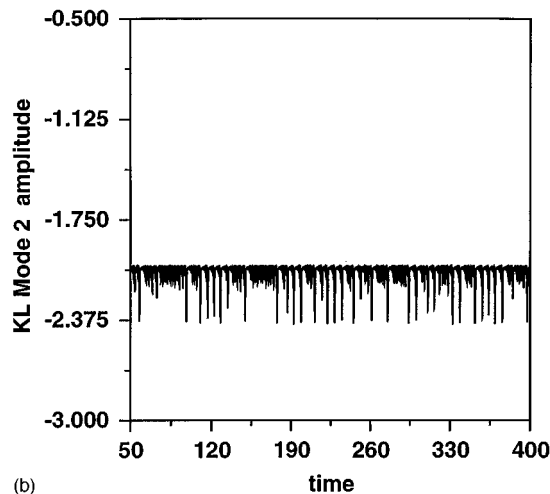
dynamics visits the upper branch of the nullcline (the so-called reduced states [15,20]).

We consider for control the time series given by the amplitude of the first KL mode. We show this time series in Fig. 6 along with the amplitude of the second KL mode.

For the system (1) the amplitude of the highest energy KL mode, (i.e., the projection of the data on this mode) captures the dynamics of the u variable, in the sense that the same bursting pattern in time is observed, i.e., growing oscillations, leading to small amplitude chaos of random length followed by a large relaxation oscillation. The amplitude of



(a)



(b)

FIG. 6. (a) Amplitude of the first KL mode for the pattern in Fig. 1. (b) Amplitude of the second KL mode for the pattern in Fig. 1.

the second mode mimics the dynamics of the v variable [Fig. 6(b)].

From the time series for $\alpha_1(t)$ we form a map by sampling the dynamics at the successive maxima. This map is shown in Fig. 4, at parameter values $D = 0.032249$, $\alpha = 0.01$, and $p = -2.0$. We can identify on this plot a fixed point of the map that corresponds to a periodic time series $\alpha(t)$. This orbit is unstable and the map is nearly one dimensional near this fixed point, so formula (6) can be used for control. In Fig. 7 we show a blowup of the dynamics near the unstable fixed point of period 1. The dynamics near the fixed point, represented by label 6, is iteratively labeled by the sequence $\dots \rightarrow 1 \rightarrow 2 \rightarrow 3 \rightarrow 4 \rightarrow \dots \rightarrow 10 \rightarrow 11 \dots$. The fixed point is a flip saddle since the iterates oscillate on alternate sides of the fixed point as they leave its neighborhood.

We identify from data the value of the fixed point and associated unstable eigenvalue and eigenvector, as well as the derivative \mathbf{g} of the fixed point with respect to the parameter p .

The algorithm acts on the solution of the reaction-diffusion system as follows: we integrate the system (1) in time and monitor the projection of the solution on the first KL mode. Every time this amplitude goes through a maximum we adjust the boundary condition (initially set at $p = -2.0$) according to formula (6). The stabilized pattern is

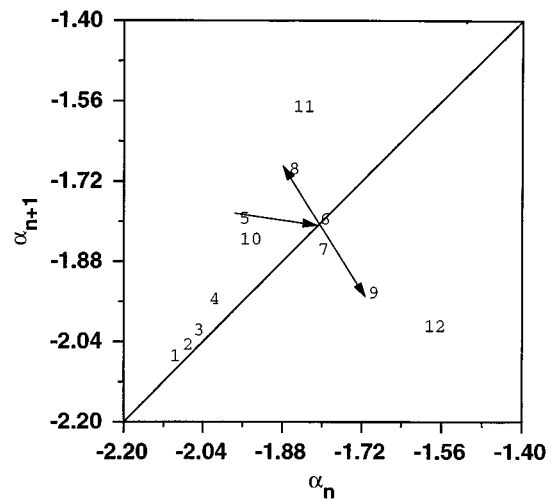


FIG. 7. Blowup of the dynamics near the unstable period-one fixed point in Fig. 4. Numbers indicate order of the iterate. Although the local dynamics appears to have an attracting direction since the nonlinear map reinjects iterate 11 into the neighborhood of the fixed point, the map is locally one dimensional with a one-dimensional unstable manifold.

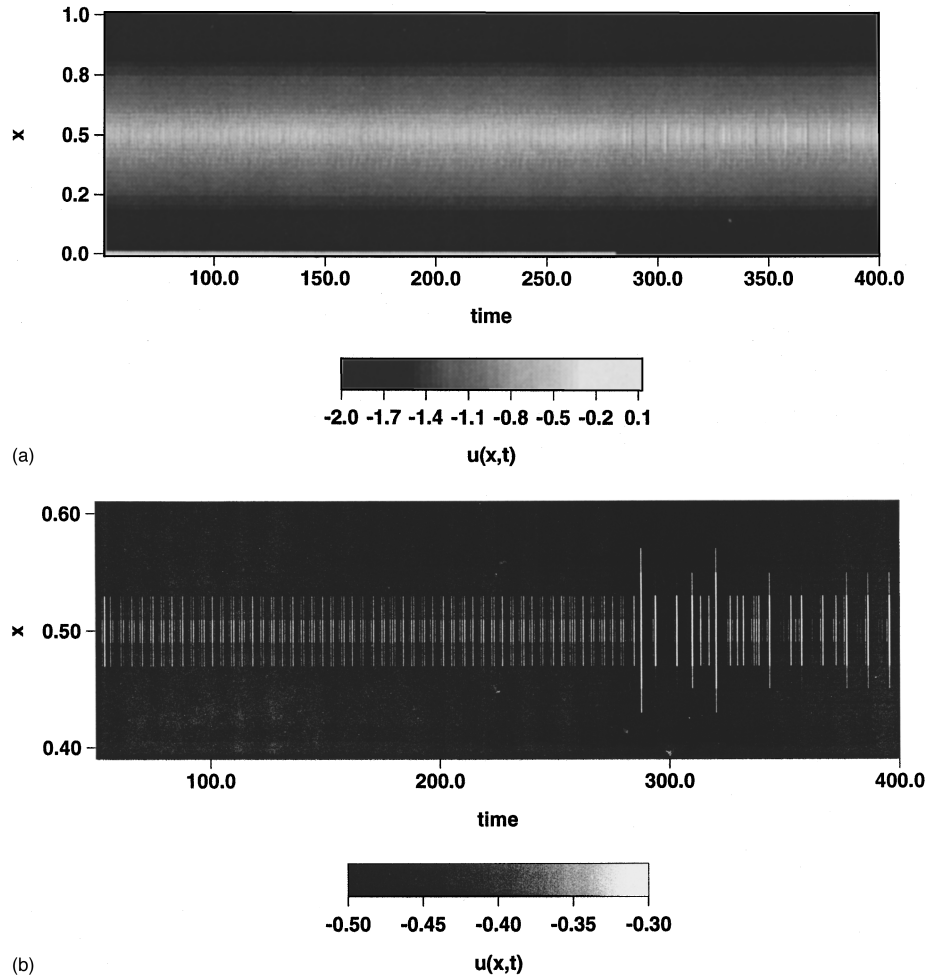


FIG. 8. (a) Stabilized pattern obtained by using KL control algorithm at the same parameter values as in Fig. 1. The control is interrupted after 250 successive bursts and the chaotic pattern returns. (b) Detailed view of the pattern in Fig. 8(a).

shown in Figs. 8(a) and 8(b). After 260 iterates we release the control and the chaotic pattern is reestablished. The amplitude of the main KL mode in this experiment is shown in Fig. 9. In Fig. 10 we show the parameter fluctuations used at the boundary to obtain the stabilized pattern in Figs. 8(a) and 8(b). For comparison we show in Fig. 11 the parameter fluctuations

used in our previous method [12], at $p = -1.3$. We notice that in the new method the parameter fluctuations are one order of magnitude smaller. Another advantage is that the control locks much faster on the desired orbit without going through large amplitude bursts in the parameter before it locks on the desired orbit. When basing the control on a

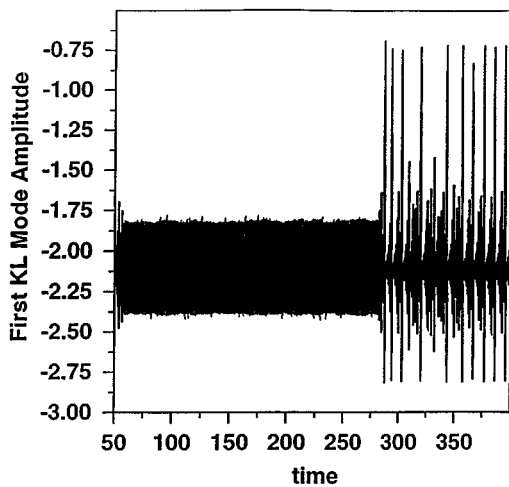


FIG. 9. Amplitude of the first KL mode while control is being active corresponding to the pattern in Fig. 8.

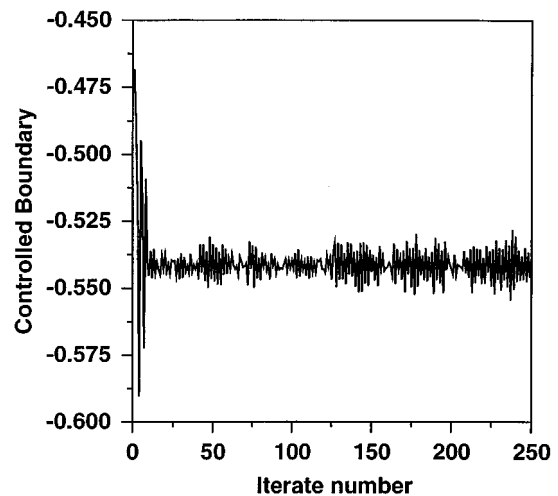


FIG. 10. Adjustments in the feed rate used to obtain the controlled pattern in Fig. 8.

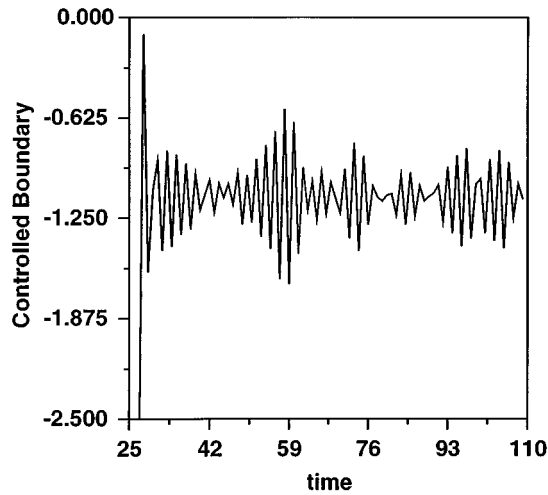


FIG. 11. Adjustments in the feed rate used for controlling periodic bursting at $p = -1.3$, when the control method is based on local measurements [12]. The control fluctuations are one order of magnitude larger than for the KL control method which are shown in Fig. 10.

sampled time series at a fixed spatial point, the change in concentration at the boundary needs time until it propagates, by diffusion or traveling wave, and affects the monitored time series. Once this time series is stabilized, due to strong correlation in space the whole pattern is stabilized. When basing control on measuring the amplitude of the first KL mode, control is more efficient, even though the geometries of the two time series are quite similar. By controlling the amplitude of the first mode we address the spatiotemporal pattern uniformly, since most of the data (90%) lie close to the spatial structure represented by the first mode, so smaller adjustments are necessary, which act on the system much faster.

We have also applied this control method when monitoring the amplitude of the second highest energy KL mode. This is a mode that contains only 4% of the energy, and stands for a spatial structure statistically decorrelated from the first mode. We noticed that the large amplitude bursts are eliminated but the small amplitude chaos is unaffected by control. This can be explained by the shape of the modes in Fig. 2. We notice that the first mode has a high peak in the first component and a low peak in the second component. That tells us that most of the data in the high bursts in the u variable and most of the data in the small amplitude chaos of the v variable are captured by this mode. The second KL mode has a high peak in both components, which indicates that data related to the high amplitude bursts are contained in this spatial structure; no information about the small amplitude chaos is contained in this mode.

VI. DISCUSSION

We have introduced a method for stabilizing unstable states of spatiotemporal processes and applied it to a reaction-diffusion equation. The method combines reconstructing the dynamics from time series, with Karhunen-Loeve mode representation of spatiotemporal data. We have showed that we can control the chaotic bursting in a model

of a chemical process by controlling the amplitude of the highest energy KL mode.

One feature of the KL control method is that it does require more data than other low-dimensional control methods, even though a time series approach is used to reconstruct the relevant phase space. Specifically, to extract the relevant modes for control, the spatial data must be sampled over a sufficiently large time interval. The solution at a second parameter is also necessary to obtain the derivative of the controlled state with respect to the parameter. However, given the improved state of the art in data taking and computational efficiency, for certain problems such as the reaction-diffusion experiments presented in [19], we feel the approach is well within the limits of feasibility.

Another feature of the KL method of control pertains to the propagation of control pulses into the medium. The reaction-diffusion problem considered is one that operates far from equilibrium state determined by the solution of the nullclines $v = f(\alpha)$ and $u = \alpha$. Nonequilibrium conditions are created by placing the boundary conditions far from the equilibrium state, which in turn sets up a gradient in the system. A gradient in reaction-diffusion systems is one mechanism that may generate traveling waves [27]. Therefore, when a control pulse is applied at the boundary, one

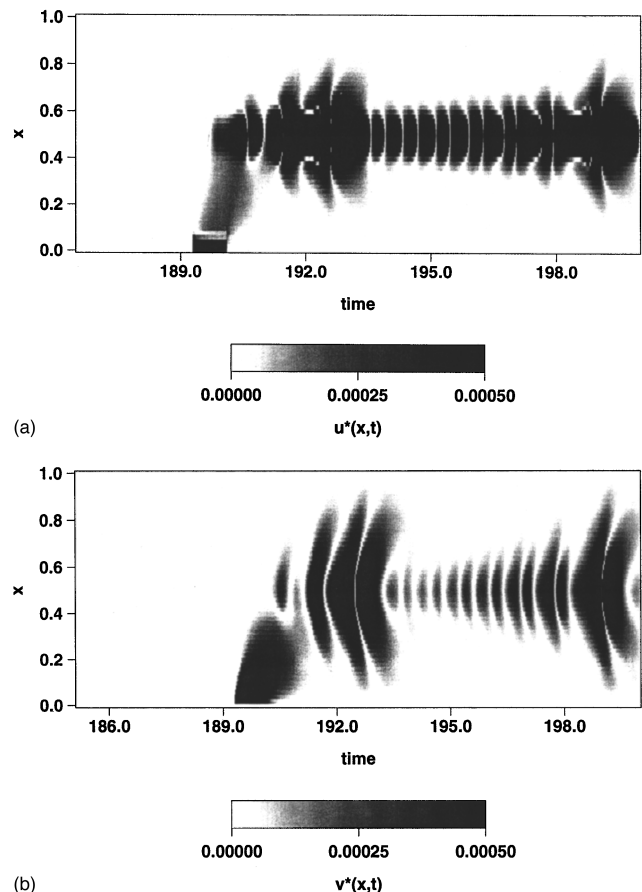


FIG. 12. The spatiotemporal pattern generated when we take the difference (u^*, v^*) between the chaotic solution and the same chaotic solution with a pulse at the boundary during a single cycle. (a) the difference in the u variable u^* . (b) the difference in the v variable v^* .

expects a wave to be generated as a result of diffusion and reaction.

The way control affects the solution can be understood by looking at a single pulse in the control parameter (i.e., one of the boundary conditions), which is kept on for an entire cycle. We plotted in Figs. 12(a) and (b) the difference (u^*, v^*) , between the solution with a single pulse and the chaotic solution without a pulse. This plot reveals the contribution of a single pulse to the spatiotemporal pattern. We notice the pulse generates a traveling wave that propagates inside the domain for the u variable. This behavior is distinct from the case where only diffusion is present (case not shown). Changes in the boundary condition are felt in the center of the domain very quickly, almost instantaneously. In the v variable, u acts as a source term, and diffusion dominates.

One of the interesting questions about using KL mode expansion for dynamics control is how many KL modes are sufficient for effective control. One can, in theory, project the original model onto all KL modes which results in a set,

albeit large, of coupled nonlinear ODE's. However, embedding theory states that all relevant information from all modes is contained in the amplitude of a single mode. This amplitude is then embedded in an appropriate space. When the dynamics can be embedded in a space of relatively low dimension, it is natural to use time series embedding methods for analysis and control.

Finally, the method we present is more robust than previous methods [12,6] in that it does not require special placement of time series measurements and control adjustments are one order of magnitude smaller. Presently we are investigating the extension of the method to models where the unstable dynamics is higher dimensional.

ACKNOWLEDGMENTS

The authors gratefully acknowledge Dr. Robert Handler and Dr. Larry Sirovich for useful discussions that led to this work. We also acknowledge the support of the Office of Naval Research for conducting this research.

-
- [1] Edward C. Ott, Celso Grebogi, and James A. Yorke, *Phys. Rev. Lett.* **64**, 1196 (1990).
 - [2] E. Ott and M. Spano, *Phys. Today* **48**, 34 (1995); T. Shinbrot, *Nonlinear Sci. Today* **3**(2), 1 (1993); T. Shinbrot, C. Grebogi, E. Ott, and J. A. Yorke, *Nature (London)* **363**, 411 (1993).
 - [3] Zelda Gills, Christina Iwata, Rajarshi Roy, Ira Schwartz, and Ioana Triandaf, *Phys. Rev. Lett.* **69**, 3169 (1992); R. Roy, T. W. Murphy, T. D. Maier, Z. Gills, and E. R. Hunt, *ibid.* **68**, 1259 (1992).
 - [4] J. Tang and H. H. Bau, *Phys. Rev. Lett.* **70**, 1795 (1993).
 - [5] M. E. Bleich and J. E. S. Socolar, *Phys. Rev. E* **57**, R16 (1996); M. E. Bleich, D. Hockheiser, J. V. Monloney, and J. E. S. Socolar, *ibid.* **55**, 2119 (1997).
 - [6] Th. Pierre, G. Bonhomme, and A. Atipo, *Phys. Rev. Lett.* **76**, 2290 (1996).
 - [7] D. S. Broomhead and G. P. King, *Physica D* **20**, 217 (1986).
 - [8] F. Takens, in *Dynamical Systems and Turbulence*, edited by D. A. Rand and L.-S. Young, Lecture Notes in Mathematics Vol. 898 (Springer-Verlag, Berlin, 1981), pp. 366–381.
 - [9] Ira Schwartz and Ioana Triandaf, *Phys. Rev. A* **46**, 7439 (1992).
 - [10] Ioana Triandaf and Ira Schwartz, *Phys. Rev. E* **48**, 718 (1993).
 - [11] Thomas L. Carroll, Ioana Triandaf, Ira Schwartz, and Lou Pecora, *Phys. Rev. A* **46**, 6189 (1992).
 - [12] Ira Schwartz and Ioana Triandaf, *Phys. Rev. E* **50**, 2548 (1994).
 - [13] Q. Ouyang, V. Castets, J. Boissonade, J. C. Roux, P. DeKepper, and H. L. Swinney, *J. Chem. Phys.* **95**, 351 (1991).
 - [14] Q. Ouyang, J. Boissonade, J. C. Roux, and P. DeKepper, *J. Chem. Phys.* **95**, 351 (1991).
 - [15] J. Elezgaray and A. Arneodo, *Phys. Rev. Lett.* **68**, 714 (1992).
 - [16] Lawrence Sirovich, *Q. Appl. Math.* **XLV**, 561 (1987).
 - [17] Ira Schwartz and Ioana Triandaf, *Chaos* **6**, 229 (1996).
 - [18] Michael D. Graham and Ioannis G. Kevrekidis, *Comput. Chem. Eng.* **20**, 495 (1996).
 - [19] F. Qin, E. E. Wolf, and H.-C. Chang, *Controlling Thermal Front Propagation on a Catalytic Converter through Video Feedback*, Proceedings of the 1993 American Control Conference—Acc'93 (American Autom. Control Council, Evanston, IL, 1993), Vol. 2, pp. 1302–1306; *Phys. Rev. Lett.* **72**, 1459 (1994).
 - [20] A. Arneodo and J. Elezgaray, in *Spatial Inhomogeneities and Transient Behavior in Chemical Kinetics*, edited by P. Gray, G. Nicolis, F. Baras, P. Borckmans, and S. K. Scott (Manchester University, Manchester, 1990), p. 415.
 - [21] K. Karhunen *Ann. Acad. Sci. Fennicae* **34**, Ser. A1, 37 (1946).
 - [22] M. M. Loeve, *Probability Theory* (Van Nostrand, Princeton, NJ, 1955).
 - [23] E. N. Lorenz, *Empirical Orthogonal Functions and Statistical Weather Prediction* (MIT, Cambridge, 1956).
 - [24] J. L. Lumley, *Stochastic Tools in Turbulence* (Academic, New York, 1970).
 - [25] G. Berkooz, P. Holmes, and J. L. Lumley, *Annu. Rev. Fluid Mech.* **25**, 539 (1993).
 - [26] F. Riesz and B. Sz. Nagy, *Functional Analysis* (Ungar, New York, 1955).
 - [27] G. B. Whitman, *Linear and Nonlinear Waves* (John Wiley and Sons, New York, 1974).